Eur. Phys. J. B **1**, 189–196 (1998)

THE EUROPEAN PHYSICAL JOURNAL B

Thermodynamics and X-ray studies of 2-alcohol monolayers at the air water interface

A. Renault[1,a], C. Alonso[1], F. Artzner[2], B. Berge[1], M. Goldmann[3], and C. Zakri[1]

[1] Laboratoire de Spectrométrie Physique[b], Université Joseph Fourier-CNRS, BP 87, 38402 St Martin d'Hères, France
[2] Laboratoire de Physique des Solides[c], Université Paris-Sud, Bat. 510, 91405 Orsay Cedex, France
[3] Laboratoire de Physico-Chimie des Surfaces et Interfaces, Institut Pierre et Marie Curie, 11 rue P. et M. Curie, 75005 Paris, France

Received: 11 April 1997 / Revised: 18 August 1997 / Accepted: 9 October 1997

Abstract. We investigate monolayers of 2-alcohols (2-C9 to 2-C16) obtained by placing a drop of pure alcohol at the water surface. These alcohols are chiral molecules and we study the racemic mixtures. By ellipsometry and surface tension measurements we are able to characterize the 2D crystallization-melting transition with temperature. We find a first order transition. Using X-ray under grazing incidence we show that the racemic mixture crystallizes at 2D on a hexagonal cell. We find a parity effect on the lateral pressure at the transition and on the stability of the Bragg peak. We compare all results with those observed for 1-alcohols.

PACS. 61.10.-i X-ray diffraction and scattering – 64.70.Dv Solid-liquid transitions – 68.10.Cr Surface energy (surface tension, interface tension, angle of contact, etc.)

1 Introduction

The nature of 3D interactions between chiral molecules and particularly the problem of segregation has been studied for a long time [1]. Indeed an understanding of the interactions is of great importance in the fields of chemistry, physics and biology [2]. Stewart and Arnett [3] investigate the 2D interactions between chiral molecules. The common idea is that on going from 3D to 2D, the chirality dependent part of molecular interactions is enhanced: the chiral heads are all in one common plane side to side. The consequence is presumably to increase the energy difference that can exist between homochiral pairs (DD or LL) and heterochiral pairs (DL). Nevertheless it is not clear if entropy differences do not play also an important role: the freezing of orientational degrees of freedom, due to the head group pointing down in water, can be compensated by an increase of the fluctuations of the molecules along and around their long axis [4,5]. These fluctuations can indeed hinder the chiral recognition between neighboor molecules. Andelman *et al.* [6] proposed a geometrical model concerning tripodal amphiphiles constituting a monolayer at the air water interface. They found that chiral discrimination leads to heterochiral behavior. Several systems have recently been studied at the air-water interface. They highlight simple chiral discrimination [2,7–11].

In our approach, we introduce at the air water interface very simple amphiphilic chiral molecules in order to understand the influence of chirality on 2D stacking. Recently, we have shown that short fatty alcohol monolayers could be studied by placing a drop of alcohol on a water surface [12]. The drop is spontaneously surrounded by a monolayer, keeping a finite contact angle at equilibrium. Two different forms of the alcohol are thus in equilibrium: in 3 dimensions in the bulk of the drop and in 2 dimensions in the monolayer. This technique allowed us to investigate short chain systems like 1-alcohols. We briefly recall the main results observed on monolayers of 1-alcohols [4,13]: a hexagonal crystalline phase, vertical chains in the rotator phase, first order melting-crystallization transition, the character of which decreases with the chain length.

The main difference between the 2-alcohols we investigate here and the other chiral systems quoted earlier, comes from the much shorter length (8 to 16 carbons in our case). This allows us to understand the importance of chirality in the 2D stacking because the role of chain-chain interaction is reduced by comparison with longer chains. Moreover, our knowledge of 2D stackings of 1-alcohols of the same length should enable us to compare the thermodynamic properties of monolayers and their structural organization, and then to try to analyse the role of the hydrophilic head in these short chain monolayers.

We devote this paper to racemic mixtures of 2-alcohols. In fact, it is necessary to characterize the behavior and

[a] e-mail: Anne.RENAULT@ujf-grenoble.fr
[b] UMR 5588
[c] URA 2

the nature of racemic mixtures before analysing the role of chirality in the 2D stacking. In a first part, we characterize the 3D melting-crystallization transition by DSC and the 2D melting-crystallization transition by ellipsometry and surface tension measurements. From the latter data we determine the melting entropy of the monolayer. Then, the first results of structural analysis done by grazing incidence diffraction of synchrotron radiation, will be described and we finish with a discussion on the comparison with 1- alcohols.

2 Experimental techniques

The racemic compounds were obtained from Aldrich SA or LANCASTER and used without further refinement. We studied 2-alcohols with chain lengths between 8 and 16 carbons. In this paper all racemic mixtures are noted 2-C12 (to take the example of dodecanol) and the enantiomer of dodecanol is denoted (S)C12. Enantiomers of even 2-alcohols were synthesized by copper-catalyzed Grignard methyl oxirane opening [14]. (S)-methyloxirane is commercially available from Sigma. (R)-methyloxirane was obtained by transformation of natural (S)-alanine [15]. In the case of octanol, studied only by DSC, we used commercial compounds for enantiomers ((S)C8, (R)C8 and 2-C8).

We used a Perkin DSC II differential scanning calorimeter to determine the melting-crystallization temperature of 2-alcohols. The sensitivity was 20 mcal s^{-1}, the quantity was ~ 5 mg, the scanning rate 10 K min^{-1} and the temperature range [120 K, 360 K].

The trough for ellipsometric and surface tension measurements was made of teflon (depth: 8 mm) and inserted in a closed metallic container regulated by circulating water. The temperature was measured by a Pt resistance in a stainless steel rod dipped into the trough. The thermal stability was about 0.05 K/hr. Surface tension was measured by a platinum Wilhemy plate weighed by a SARTORIUS balance which yielded in a stability of about 0.5 mN/m over 12 hours. For ellipsometry, a He-Ne laser followed by a GLAN-THOMPSON polarizer reflecting on the water surface through little holes in the container top was used. A null ellipsometer was built from a $\lambda/4$ wave plate, a GLAN-THOMPSON analyser and a photomultiplier. The angle of incidence was 1.00 degree away from the Brewster angle. The zero intensity was continuously monitored by means of small variations of the computer controlled polarizer and analyser rotations. In this configuration, the analyser rotation angle is half the phase difference δ between the two orthogonal polarizations.

Our X-ray experiments were carried out at the LURE Synchrotron facility (Orsay) on the D41B beam line. A monochromatic X-ray beam with a wavelength of 1.488 Å is selected by an asymmetrically cut vertical Ge(111) crystal, a slight curvature for horizontal focussing with a divergence of 1 mrad. A silica mirror is used to deflect the beam down on to the water surface at an incidence angle of 2.0 mrad. Between the mirror and the trough, the beam is collimated through Huber slits with a vertical height of

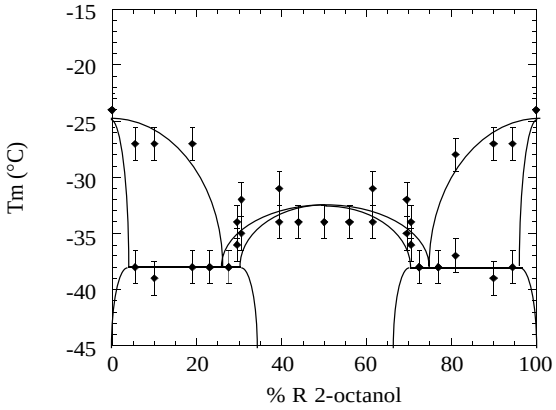

(a)

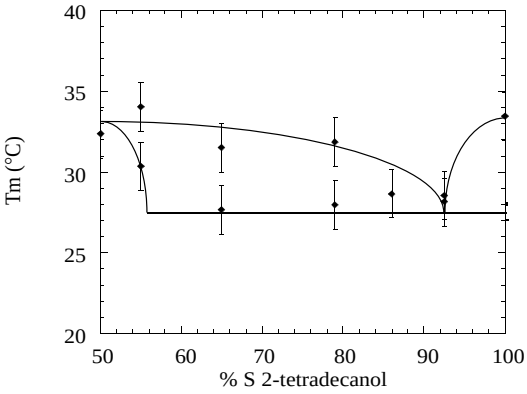

(b)

Fig. 1. Phase diagram obtained by DSC as a function of % of enantiomer. The line is not calculated (a) on 2-octanol, (b) on 2-tetradecanol.

100 μm and a width of 5 mm and the intensity of the incident beam is monitored with a pair of diodes. Scattered X-rays are counted by a circular Position Sensitive Detector (radius = 550 mm) which allows the rod scan measurements. Soller slits are used for horizontal collimation, their full angle of acceptance being 2.6 mrad. The resolution in the wave vector transfer, Q, is about 10^{-2} $Å^{-1}$ (FWHM). The integration range along q_z is from 0 to 0.4 $Å^{-1}$ owing to the vertical size of Soller slits. A special circular Teflon trough of diameter 80 mm was designed for the X-ray diffraction experiments [13]. It can rotate continuously about a vertical axis at a slow speed, in order to average the crystalline grain structure. The temperature within the trough is regulated by circulation of a thermal liquid (range of temperature [250 K − 330 K]). In order to reduce capillary waves at the water-air interface, a flat silicon block is immersed in the trough, leaving a typical thickness of 300 μm of water under the alcohol monolayer.

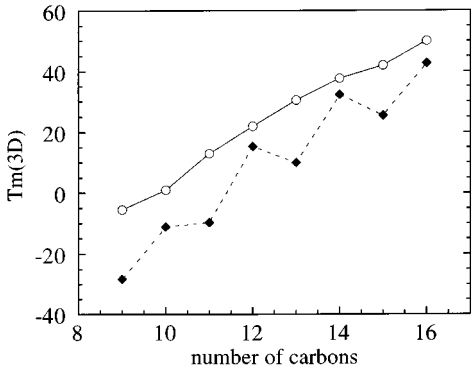

Fig. 2. Comparison of melting temperature ($T_{m(3D)}$) between 1-alcohols (o) and 2-alcohols (♦).

To preserve alignment at the water surface during long experiments, we developed a regulation system for the water level. The stability is of the order of $+/-5$ μm over several hours. For X-ray and ellipsometric measurements, all studies were performed by depositing a monolayer in its liquid phase.

3 Characterization of the 3D phase diagram

We first determined, by Differential Scanning Calorimetry (DSC), the phase diagram of the racemic mixtures for different alcohols (2-C8, 2-C10, 2-C12, 2-C13, 2-C14 and 2-C16). Two diagrams are shown in Figure 1: (a) for 2-C8 and (b) 2-C14 (in this case, we purified only (S) enantiomer). For all alcohols, this diagram is typical of a racemate (ordered mixture of left and right enantiomers). This result is not surprising because we know that 90% of racemic mixtures are racemates [16].

As explained in the introduction, a knowledge of crystallization ($T_{c(3D)}$) and melting ($T_{m(3D)}$) temperatures is essential because the monolayer is always in equilibrium with a reservoir. For all alcohols between 2-C8 and 2-C16, we performed many DSC measurements on 3D systems to determine the temperature of crystallization and of melting. The values, for 2-C9 to 2-C16, are shown in Table 1. We observed only one transition at the increase and at the decrease of temperature. This result indicates the absence of a rotator liquid crystal phase just below the melting [17]. We observed a large effect of the parity of the chains, which has already been observed in the 3D organization of 1-alcohols and alkanes [18]. In this case, we know that the parity effect is related to the orientation of chains in a structure (tilted for even chains or vertical for odd chains). In the case of 2-alcohols, although the 3D crystalline structure is unknown, we suppose that it is probably due to the orientation of chains. The effect of parity on the transition temperatures seems stronger in the case of 2-alcohols than for 1-alcohols (Fig. 2). For an equivalent chain length (same number of carbons from the OH group to the molecule's extremity), the melting temperature of the 2-alcohol is lower than that of 1-alcohol.

The melting enthalpy and entropy in the bulk are summarized in Table 1. We observed also an effect of parity of the chains. We remarked that transition enthalpy is smaller for the enantiomer than for the racemic (one example: for (S)C14, $\Delta H_m = 22$ kJ/mol and for 2-C14 $\Delta H_m = 28$ kJ/mol). The enantiomeric solid phase is therefore less stable than that of the racemic mixture. This confirms the phase diagram which is characteristic of a racemate.

4 Ellipsometry and surface tension measurements on monolayers

Figure 3a summarizes the results of ellipsometry as the temperature is decreased. A clear first order phase transition is visible for compounds with chain length from 12 to 16. A decrease is observed in the height of the jump with decreasing chain length. Figure 3b shows the surface tension measured simultaneously with the data in Figure 3a. For each compound we find a break in the slope that coincides with the jump in ellipsometry. We list in Table 2 the temperature of the 2D melting transition, no effect of the parity of chains is observed. For 2-undecanol (2-C11), the jump at the transition is small ($< 0.2°$) and no break in slope is detectable for surface tension measurements. For chain lengths smaller than 2-C10, no measurable gap is observed in ellipsometry at the transition.

Figure 3b shows the strong effect of parity on the lateral pressure at the transition. If we compare the results obtained for 2-alcohols with those obtained for 1-alcohols, we conclude that for the same number of carbons, the jump in ellipsometry is smaller for 2-alcohols and the temperature of the melting-crystallization transition is lower. In all 1-alcohols, the melting point of the monolayer, $T_{m(2D)}$, is about 15 K above that of the bulk, $T_{m(3D)}$. Nevertheless, for 2-alcohols, depending on the chain length, $T_{m(3D)}$ can be lower or higher than $T_{m(2D)}$. This result is very important because in contrast to 1-alcohols where a monolayer is in equilibrium with a liquid drop at the 2D melting transition, for 2-alcohols we can have a solid drop (2-C12, 2-C14) or a liquid drop (2-C13, 2-C15, 2-C16) at the melting transition.

By surface tension measurements, we can determine the 3D melting and crystallization temperatures. We observed that the values are closed to those obtained by DSC indicating that hydration has weak or no effect on $T_{m(3D)}$ [17].

5 Thermodynamic results concerning monolayers

As the temperature is raised, two types of behavior are observed depending on the chain lengths:

- For 2-C13, 2-C15, 2-C16, results are similar to those of 1-alcohols: the surface tension depends linearly on temperature in the solid and liquid phases with a positive slope

Table 1. Results on racemic mixtures by DSC.

Number of carbons	$(T_{m(3D)})$ (°C)	$(T_{c(3D)})$ (°C)	ΔT(°C)	ΔH_m (kJ/mol)	$\Delta S_{m(3D)}$ (k_B/molecule)
9	−29	−67	38	10	4.7
10	−15	−42	27	12	5.5
11	−14	−21	7	13	6.0
12	15	3	12	22	9.0
13	10	7	3	20	8.5
14	33	21	12	28	11.2
15	26	23	3	20	8.2
16	43	29	14	36	13.6

Table 2. Thermodynamic data on racemic mixtures of 2-alcohol monolayers. The area per molecule and ΔS_{2D} are determined by two methods described in the paper.

Number of carbons	$T_{m(2D)}$) (°C)	$(T_{c(2D)})$ (°C)	ΔT(°C)	$\Delta S_{2D} \pm 0.2$ (k_B)(1)	$\Delta S_{2D} \pm 0.2$ (k_B)(2)	$a_l \pm 1$ (Å^2/mol) (1)	$a_l \pm 1$ (Å^2/mol) (2)
12	6.2	8.1	−1.9	2.8	3.0	25.0	24.6
13	19.7	19.7	0	/	4.8	/	26.6
14	26.2	28.8	−2.6	4.9	5.3	27.5	27.2
15	36.7	36.7	0	/	6.7	/	28.6
16	44.9	44.9	0	6.9	7.2	29.1	29.2

which is reproducible upon cooling and heating. This indicates that the reservoir drop is always liquid, even though the bulk temperature is below $T_{m(3D)}$. In the latter case, the drop is supercooled.

• For 2-C11, 2-C12, 2-C14, the results are complex: the surface tension depends linearly on temperature in the solid and liquid phases with positive slopes upon cooling, and negative then positive slopes upon heating (Fig. 4). This indicates that the reservoir drop is liquid at the beginning of cooling but crystallizes during this temperature decreasing. The ellipsometric measurements also show a strong hysteresis due to crystallization of the drop. Two methods can be used to analyse the thermodynamics of this system (the area per molecule in liquid phase and also, the difference of entropy at the 2D liquid- solid transition). The first method is as follows:
At any temperature the Gibbs adsorption equation [4] describes the equilibrium of the monolayer with the 3D reservoir drop by

$$(\mathrm{d}\sigma/\mathrm{d}T) = (S_{3D} - S_{2D})/a \qquad (1)$$

where σ is the surface tension, S and a are the entropy and the area per molecule. The subscripts 3D and 2D refer to the drop and monolayer phases. In Figure 4, we show the surface tension measurements with the different phases (2D, 3D) and slopes $(\mathrm{d}\sigma/\mathrm{d}T)_i$ in a thermal cycle, where i refers to different stages of the cycle and the ellipsometric measurements during the same cycle in the case of 2-C14. We first describe this figure.

Upon cooling, drop and monolayer are liquid ($i = 1$). Crystallization of the monolayer occurs at $T_{c(2D)}$, so that the monolayer is solid and the drop is liquid ($i = 2$). Then the drop crystallizes at $T_{c(3D)}$, and the surface tension increases rapidly. Upon heating, drop and monolayer are solid ($i = 3$). The monolayer melts at $T_{m(2D)}$, so that the monolayer is liquid and the drop is solid ($i = 4$). The drop melts at $T_{m(3D)}$ and drop and monolayer are therefore liquid ($i = 5$). The negative $(\mathrm{d}\sigma/\mathrm{d}T)_4$ and equation (1) prove that the entropy of the liquid monolayer is higher than that of the solid bulk.

Hysteresis is observed in the melting-crystallization temperature of the monolayer in this case. Contrary to the well known supercooled transition of 3D solids, crystallization of the monolayer occurs at a higher temperature than its melting point as shown in Figure 4. This inversion of temperature is due to a lower surface tension upon cooling. In fact, the monolayer is in equilibrium with a drop which is in a metastable state. At T below $T_{m(3D)}$ the chemical potential of the metastable liquid phase, $\mu_{3Dliq(1)}$ is higher than the chemical potential of the stable solid phase, $\mu_{3Dsol(4)}$. Although the drop is in a metastable phase, we can assume that the chemical potential of the monolayer μ_{2D} is equal to the chemical potential of the drop μ_{3D}. $\mu_{2D(1)}$ is therefore larger than $\mu_{2D(4)}$, and from the equation of state of the monolayer:

$$a\mathrm{d}\sigma + \mathrm{d}\mu_{2D} + S_{2D}\mathrm{d}T - V_{2D}\mathrm{d}P = 0 \qquad (2)$$

the following relation is derived:

$$(\partial\mu/\partial\sigma)_{T,P} = -a$$

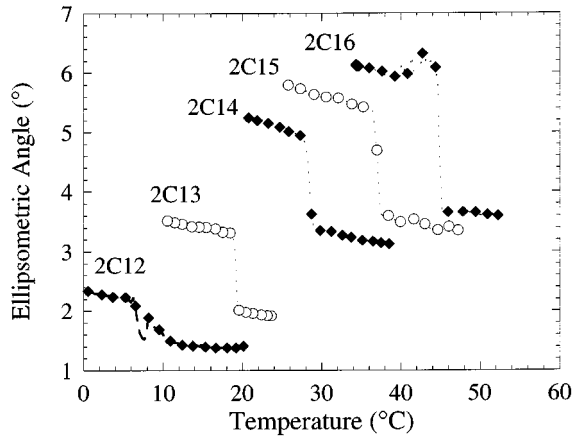

(a)

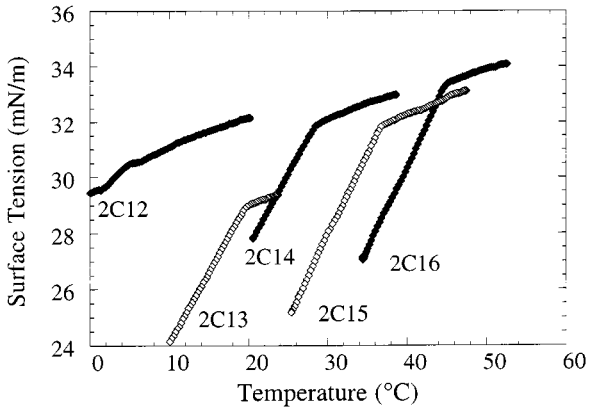

(b)

Fig. 3. (a) Ellipsometric angle of 2-alcohol monolayers (2-C12 to 2-C16) *versus* temperature. (b) Surface tension measurements of the same samples as in (a).

which on integration over σ at constant T gives the following result:

$$\mu_{2D(1)} > \mu_{2D(4)} \longleftrightarrow \sigma_{2D(1)} < \sigma_{2D(4)}.$$

The surface tension is therefore lower during cooling because the reservoir drop is in the supercooled liquid phase rather than in its stable crystalline phase.

The melting of the reservoir drop upon heating allows us to calculate the area per molecule within the monolayer. If we substract the slopes (4) and (5), the following relation is obtained at $T_{m(3D)}$

$$(d\sigma/dT)_4 - (d\sigma/dT)_5 = (S_{3Dliq} - S_{3Dsol})/a_l \qquad (3)$$

$(S_{3Dliq} - S_{3Dsol})$ was evaluated from DSC measurements and the slopes are obtained from Figure 4. The area per molecule in the liquid phase are calculated and thus, knowing a_l, we can evaluate ΔS_{2D} of the monolayer [19]. All results are summarized in Table 2.

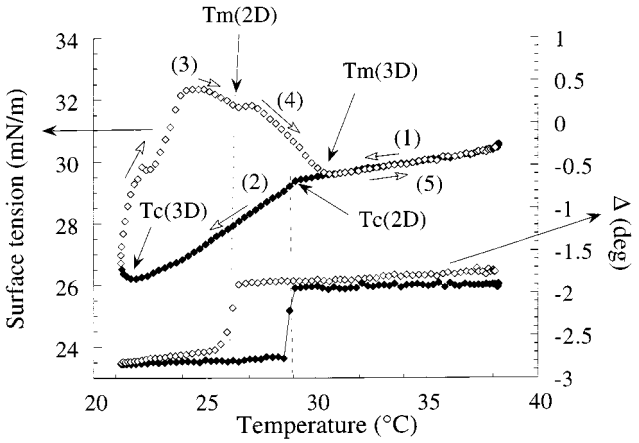

Fig. 4. Variation of the surface tension and ellipsometric angle during a temperature cycle for 2-tetradecanol monolayer in equilibrium with a drop of pure alcohol. Arrows indicate the temperature variation.

The second method uses the dilution of the alcohol drop in an alkane and Clapeyron formulae [4]:

$$(d\sigma/dT)_t = \Delta S_{2D}/(a_s - a_l). \qquad (4)$$

If the alcohol is mixed with an alkane in the reservoir drop, the surface pressure of the alcohol monolayer decreases and as shown in [4], the entropy of melting ΔS_{2D} and the area per molecule in the liquid phase a_l can be determined. For all the alcohols, a coexistence line was found, the slope of which was: -1.30 ± 0.1 mN/K, and we fixed the area per molecule in the solid phase, a_s, at 21.5 Å^2/mol (determined by X-ray). The results are summarized in Table 2. Figure 5 shows the results for the entropy of melting ΔS_{2D} (Fig. 5a) and the area per molecule in the liquid phase a_l (Fig. 5b) as a function of n (number of carbon atoms).

The results for the area per molecule in the liquid phase and for ΔS_{2D} are very similar in both methods. We conclude that these data are reliable.

As in the case of 1-alcohols, ΔS_{2D} and $(a_s - a_l)$ both indicate that the first order character of the transition is expected to vanish for $n < 9$. For the same number of carbons, the entropy at the 2D transition is smaller for 2-alcohols than for 1-alcohol monolayers (Tab. 3). The difference is $\sim 1\ k_B$/mol.

The difference measured between 1- and 2-alcohols seems to prove that the CH_3 group close to OH play a minor role in the properties of the monolayer but only the chain length and the anchoring of the hydroxyl group are very important. PM- IRRAS measurements seem to show that the polar head blocks more degrees of freedom because it is harder for the hydroxyl group to orientate towards water [20].

6 Crystal structure of the monolayers

We analyse by grazing incidence diffraction the solid phase of monolayer. For all chain lengths, we observe only one

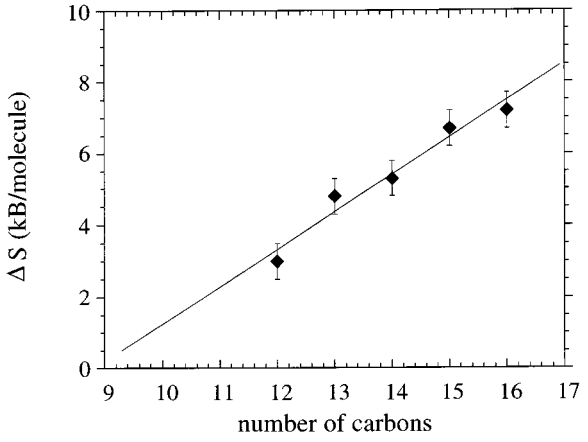

(a)

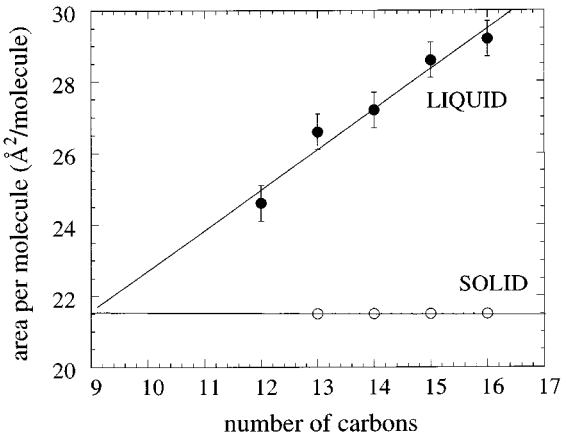

(b)

Fig. 5. (a) Calculated values of the monolayer entropy of melting ΔS_{2D} as a function of number of carbons (n). (b) Area per molecule in liquid phase a_l (closed circles) and in solid phase a_s (open circles, from X-ray data) as a function of number of carbons (n).

peak. Its intensity and line shape are different from one compound to another. The width of the peak and the line shape were analysed in terms of Lorentzian curves and also by a power law [13] $S(Q) \sim (Q - Q_o)^{-(2-\eta)}$. All data concerning X-ray measurements are summarized in Table 3.

In the case of 2-hexadecanol and 2-pentadecanol, studies show a behavior similar to that observed for 1-alcohol monolayers. We observe a very sharp peak with a coherence length greater than 2000 Å, which disappears suddenly at the transition. The analysis of the rod scans show that the 2D solid phase is a hexagonal rotator phase. The power law fit [13] gives a vanishing exponent η, as for a Lorentzian curve. The thermal expansion coefficient of the cell is $\sim 1.3 \times 10^{-3}$ Å^{-1} K^{-1}, nearly the same as that observed for 1-alcohols.

Table 3. Comparison between 1-alcohols and 2-alcohols. X-ray (hexagonal cell parameter and the coherence length) and entropy (ΔS_{2D} and $T_{m(2D)}$) results. (It has been noted that we have no measurement concerning 1-C15).

	$T_{m(2D)}$ ± 1 °C	ΔS_{2D} $\pm 0.5\ k_B$	a_{hex} ± 0.005 Å $(T_{M(2D)} - T)$	L ± 200 Å $(T_{M(2D)} - T)$
1-C12	39.5	3.6	4.936 (9.0)	> 2000 (9.0)
2-C12	7.0	3.0	4.964 (9.0)	> 300 (9.0)
1-C13	48.0	5.3	5.010 (3.5)	> 2000 (3.5)
2-C13	20.0	4.8	4.975 (2.9)	1500 (2.9)
1-C14	55.0	6.4	4.980 (4.5)	> 2000 (4.5)
2-C14	28.5	5.4	4.956 (3.9)	500 (3.9)
2-C15	36.0	6.7	4.983 (3.7)	> 2000 (3.7)
1-C16	67.0	8.0	4.962 (3.0)	> 2000 (3.0)
2-C16	45.0	7.2	4.963 (3.5)	> 2000 (3.7)

In the case of 2-tridecanol, we observe also one peak with a shorter coherence length than that observed above, about 1500 Å. The expansion coefficient is of the same order of magnitude and the intensity decreases quickly at the melting point (Fig. 6a). The power law analysis yields a η close to 0.3 with little temperature variation. The analysis of the rod scan (Fig. 6a in insert) shows a maximum at $q_z = 0$. In consequence, we can assume a hexagonal rotator phase but with a weaker positional long range order.

In the case of 2-tetradecanol, we observed one peak with a maximum at $q_z = 0$, that corresponds to a hexagonal cell (Fig. 6b). Nevertheless, the coherence length determined by the fit is short (~ 500 Å). This result seems to show that in the case of 2-C14 (and also for 2-C12), we have probably a hexatic phase.

Moreover, for these two compounds, we observed a time shift of the Bragg peak at constant temperature. These effects can be due to 2D fluctuations or thermodynamic equilibrium. The first explanation is related to a disordering of the monolayer as a result either of a solid solution or of a kinetics. For the second one, we knew that, in the case of these alcohols, the drop is solid during the passage through the melting-crystallization transition of the monolayer. One hypothesis could be that the drop is

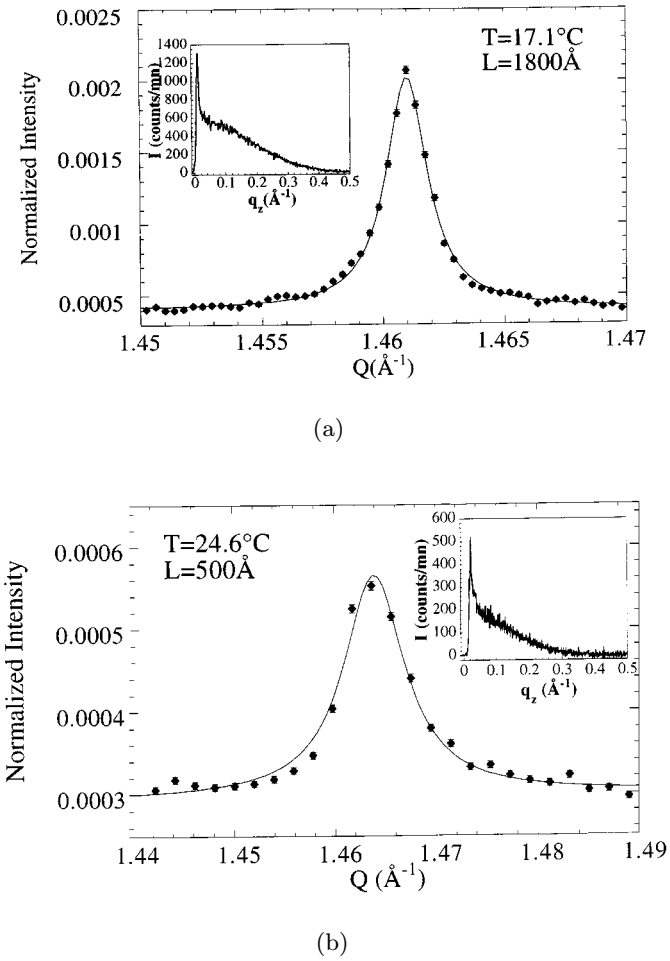

Fig. 6. (a) Bragg peak of 2-tridecanol monolayer at fixed temperature $T = 17.0$ °C (in insert: observed Bragg rod intensity profiles of the peak). (b) Bragg peak of 2-tetradecanol monolayer at fixed temperature $T = 24.6$ °C (in insert: observed Bragg rod intensity profiles of the peak).

no longer a reservoir for the monolayer and the monolayer should transform again. To overcome this difficulty, we diluted the alcohol in a ramified alkane (Squalane) in order to lower the crystallization temperature of the drop. We observed exactly the same phenomenon. To try to understand this, ellipsometry and surface tension measurements were carried out in the same conditions as the diffraction experiments. They show that the monolayer is still in a phase having the ellipsometric responses typical of a solid phase, although the surface pressure decreases.

In conclusion, we observe from these diffraction experiments that the coherence length decreases as the chain length decreases. This result seems to prove that the head does not naturally adopt a hexagonal lattice and as the influence of the head becomes more and more important as the length of the chains decreases, it destabilizes the long range order.

We have differences between 1-alcohols and 2-alcohols (Tab. 3). First of all, we have a parity effect on coherence length for shorter chains (2-C15 to 2-C12). For 2-C15 and 2-C13 we measured values closed to those obtained for 1-alcohols. On the other hand, for even short chains the values are smaller. We observed, also, an effect of parity (for $n < 16$) on the stability of the monolayer in the hexagonal phase for 2-alcohols.

If we compare the cell parameter of the two families (Tab. 3), we noted that the values are close and a parity effect in each family of alcohol.

7 Discussion

We know that if the area per molecule decreases, the entropy at the transition decreases [19]. This remark and the fact that, for identical carbon number the chain is smaller for 2-alcohols, explain why the tendancy towards second order is stronger for 2-alcohols than for 1-alcohols. This analysis is confirmed by the entropy calculations and by the calculation of area per molecule in the liquid phase. The entropy of melting seems to be systematically lower for 2-alcohols than for 1-alcohols, by a value of $\sim 1(k_B/\text{mol})$ corresponding more or less to the entropy of one extra CH_2-CH_2 bond. This shows that the important parameter is the number of bonds between the OH group and the chain extremity. For example, the melting behavior (jump in ellipsometry, ΔS_{2D}) of 2-C14 and 1-C13 are similar to each other.

The X-ray study shows that for racemic mixtures only one peak is observed with a hexagonal cell parameter about 5 Å. This value corresponds perfectly to the close packing of chains for rotator phase. This crystalline phase is similar to that of 1-alcohols although the head plays a more important role. A different behavior is however observed: the stability, time dependence and also the coherence length are strongly dependent on the length and on the parity of the chains.

The behavior observed for racemic mixtures of even alcohols 2-C12 and 2-C14 is surprising. This seems to show that the monolayer is in a dense disordered phase (denser than the liquid), probably even more disordered than mesophases precently observed in fatty acids [21].

8 Conclusion

We were able to show that racemic 2-alcohols mixtures form in 3D racemates. A strong parity effect takes place for the 3D melting temperatures but not in 2D. Racemic mixtures of the 2-alcohols exhibit a hexagonal rotator phase at 2D. The thermodynamic and structure properties of racemic mixtures of 2-alcohols are similar to those of 1-alcohols. Nevertheless, in the monolayer, the parity of the chains seems to have an effect on the transition pressure, on the crystal structure and also on the stability of the hexagonal phase. The two last points correspond to the important difference between 1-alcohol and 2-alcohol

monolayers. Probably for the shorter chains, we tend to a weak first order transition with an increase of 2D fluctuations in the solid phase.

It should be recall that contrary to 1-alcohol, in the case of 2-alcohol, we have a mixture of two types of molecules (left and right molecules). Perhaps, the difference observed between 1-alcohols and 2-alcohols monolayers is due to this fact.

Our current structural and thermodynamic studies of the enantiomers will enable us to determine the structure of the racemic mixture in 2D, conglomerate or racemate or solid solution.

We would like to acknowledge fruitful discussions with Janine and Joseph Lajzerowicz and thank Mr Gerard Commandeur for his help during DSC measurements.

References

1. J. Jacques, A. Collet, S.H. Wilen, *Enantiomers, racemates and Resolutions* (Wiley Ed., New York, 1981).
2. R.M. Weis, H.M. Mc connell, J. Phys. Chem. **89**, 4453 (1985).
3. E.M. Arnett, J. Chao, B.J. Kinzig, B.J. Stewart, O. Thompson, R.J. Verbiar, J. Am. Chem. Soc. **104**, 389 (1982); J.G. Heath, E.M. Arnett, J. Am. Chem. Soc. **114**, 4500 (1992) and references cited therein.
4. B. Berge, O. Konovalov, J. Lajzerowicz, A. Renault, J.P. Rieu, M. Vallade, J. Als-Nielsen, G. Grübel, J.F. Legrand, Phys. Rev. Lett. **73**, 1652 (1994) and references therein.
5. A.V. Tkachenko, Y. Rabin, Phys. Rev. Lett. **76**, 2527 (1996).
6. D. Andelman, P.G. De Gennes, C.R. Acad. Sci. Paris **307**, 233 (1988).
7. J.T. Groves, H. Mc Connell, Biophys. J. **70**, 1573 (1996).
8. F. Bringezu, G. Brezesinski, P. Nuhn, H. Möhwald, Biophys. J. **70**, 1789 (1996).
9. E. Scalas, G. Brezezinski, H. Möhwald, V.W. Kaganer, W.G. Bouwman, K. Kjaer, Thin Solid Films **284**, 56 (1996).
10. D. Jacquemain, S. Grayer-Wolf, F. Leveiller, M. Deutsch, K. Kjaer, J. Als Nielsen, M. Lahav, L. Leiserowitz, Angew. Chem. Int. Ed. Eng. **31**, 130 (1992).
11. P. Nassoy, M. Goldmann, O. Bouloussa, F. Rondelez, Phys. Rev. Lett. **75**, 457 (1995).
12. B. Berge, A. Renault, Europhys. Lett. **21**, 773 (1993).
13. C. Zakri, A. Renault, J.-P. Rieu, M. Vallade, B. Berge, J.F. Legrand, G. Vignault, G. Grübel, Phys. Rev. B **55**, 14 163 (1997).
14. A.A. Kandil, K.N. Slessor, Can. J. Chem. **61**, 1166 (1983).
15. B. Koppenhoefer, V. Schurig, Org. Synth. **66** 151 (1987); B. Koppenhoefer, V. Schurig, Org. Synth. **66**, 160 (1987).
16. C.P. Brock, W.B. Schweizer, J.D. Dunitz, J. Am. Chem. Soc. **113**, 9811 (1991).
17. E.B. Sirota, X.Z. Wu, J. Chem. Phys. **105**, 7763 (1996).
18. D. Small, *The Physical chemistry of Lipids, Handbook of Lipid Research*, **4** (Plenum Press, NY, 1986).
19. J.P. Rieu, M. Vallade, J. Chem. Phys. **104**, 7729 (1996).
20. C. Alonso, D. Blaudez, F. Artzner, B. Desbat, B. Berge, A. Renault, submitted to Chem. Phys. Lett (July 1997).
21. R. Kenn, C. Bohm, A. Bibo, I.R. Peterson, H. Möhwald, K. Kjaer, A. Als-Nielsen, J. Phys. Chem. **95**, 2092 (1991).